Fizika Nizkikh Temperatur, 2006, v. 32, No. 6, p. 746–752

Localization effects and pseudogap state in $YBa_2Cu_3O_{7-}$ single crystals with different oxygen content

M.A. Obolenskii, R.V. Vovk, A.V. Bondarenko, and N.N. Chebotaev

V.N. Karazin Kharkov National University, 4 Svoboda sq., Kharkiv, 61077, Ukraine
E-mail: ruslan.v.vovk@univer.kharkov.ua

Received November 10, 2005, revised February 13, 2006

We have investigated the evolution of the temperature dependence of the in-plane and off-plane conductivity of $YBa_2Cu_3O_{7-\delta}$ single crystals due to the decrease of the oxygen content in the samples caused by a heat treatment. The concentration dependence of the in-plane and off-plane energy gaps has been determined. It has been shown that the enhancement of the localization effects results in a suppression of the pseudogap state. At the same time, the decrease of the oxygen content results in a relative narrowing of the temperature interval in which the regime of the fluctuating conductivity is realized.

PACS: 74.72.Bk

Keywords: $YBa_2Cu_3O_{7-\delta}$ single crystals, preudogap, localization, oxygen content, crossover.

It is well known that the decrease of the oxygen content in high-temperature superconducting (HTSC) compounds $YBa_2Cu_3O_{7-\delta}$ results in significant qualitative changes of the temperature dependence of the electroresistance $\rho(T)$. At the same time, there is a principal difference between the behavior of the electroresistance measured in the *ab* plane ($\rho_{ab}(T)$) and parallel to axis **c** ($\rho_c(T)$) [1,2]. A small change in the oxygen stehiometry results in a transition from the metallic behavior of curves $\rho_c(T)$ to that with a typical thermoactivated bending. In contrast, a wide linear region is persisted in $\rho_{ab}(T)$ at relatively high temperatures even at significant deficiency of oxygen $\delta > 0.3$, which is a signature of a stable intensity of scattering of normal carriers [3]. When the temperature is reduced below some typical value T^* [4] a deviation of $\rho_{ab}(T)$ from the linear dependence occurs, which is an evidence of the presence of some excess conductivity that may be caused by a transition to the pseudogap (PG) regime. Two different scenarios for the PG anomaly in HTSC systems have been intensively discussed in the literature. According to the first one, the PG regime is connected to short-range fluctuations of a «dielectric» type existing in underdoped compounds (for a review see [5]). The second scenario assumes that Cooper pairs are formed already at temperatures much higher than the critical temperature $T^* >> T_c$, while their phase coherence is established only at $T < T_c$ [6,7]. Despite the extensive experimental material collected by now, this question remains unresolved. This is partially due to the fact that the most of the experimental studies were performed with ceramic, textured and film samples obtained by rather different technological processes (see, for example, [6–9]). Here we report results of the investigation of the evolution of the various regimes of the conductivity in the *ab* plane and along the **c** axis within high-quality single crystals of Y–Ba–Cu–O subjected to a stage-by-stage oxygen removal by a heat treatment.

The single crystals of $YBa_2Cu_3O_{7-\delta}$ were grown in a gold crusible at the temperature of 850–970 °C by means of the self-flux method as it was described in detail in [1,2]. The characteristic sizes of samples were 2×0.3×0.02 mm for the measurements in the *ab* plane, and 0.3×0.5×0.1 mm for the measurements parallel to the **c** axis. The smallest dimension of a crystal corresponded to the **c** axis. To obtain samples with an optimal oxygen content ($\delta < 0.1$), the crystals were annealed in an oxygen flow at the temperature of 400 °C for five days. To further reduce the oxygen content, the samples were oxygen annealed at higher temperatures for three to five days. The parameters of the investigated samples are shown in the Table.

Table. Parameters of the samples

7−δ	T_a	T_c^{ab}	$\rho_{ab}(300)$,	$\rho_c(300)$,	T^*	Δ_c		Δ^*_{ab}	
	K		μOhm·cm	mOhm·cm	K	K	meV	K	meV
6.92	670	91.74	155	11.625	143	118	10.14	1033	89.05
6.87	720	90.85	186	14.205	171	170	14.67	812	70
6.83	760	88.71	192	19.266	192	225	19.41	599	51.64
6.81	790	87.89	216	37.487	215	308	26.54	469	40.43
6.77	810	78.52	243	44.247	232	346	29.85	290	25
6.65	890	57.45	558	139.5	253	450	38.81	71	6.12
6.45	950	45.11	1963	–	–	–	–	–	–

Silver electrocontacts were connected to the surface of the crystals by means of the silver paste. The electroresistance was measured using the standard four-contact method for two opposite directions of a dc current of 1 mA at a zero magnetic field. In addition, the sample geometry was such that the vector of the transport current was at an angle of 45° to the plane of the twin boundaries (TB). The temperature was measured by a copper-constantan thermocouple, and the voltage on a sample and the sample resistance was measured by nanovoltmeter V2-38. The data from the voltmeters were automatically transferred to a computer. The temperature was drifting during the measurements, with the drift being about 0.1 K/min near T_c and about 5 K/min at $T > T_c$. The critical temperature was determined as a midpoint of superconducting transition. All measurements were made in three days after the annealing, which ensured an equilibrium oxygen distribution within the sample at room temperature [2].

The dependences of $\rho_c(T)$ measured after the sample annealing at different temperatures are shown in Fig. 1,*a* (the resistive transitions to the superconducting state are shown in Fig. 1,*b*). One can see that increase of the annealing temperature results in decrease of T_c and in a transition of curves $\rho_c(T)$ from a metallic behavior to that with a characteristic semiconductor deflection. In Fig. 1,*c* and *d* the same dependences are shown in coordinates $\ln(\rho/T^{1/2})-1/T^4$ and $\ln(\rho/T)-1/T$, which corresponds to the description of function $\rho_c = f(T)$ by means of analytical expressions:

$$\rho_c = AT\exp(\Delta/T) \quad \text{and} \quad \rho_c = BT^{1/2}\exp(T_0/T)^{1/4}, \tag{1}$$

where A, B, and T_0 are constants; Δ is the activation energy. It is known that the first expression is typical for the activation mechanism of the carrier motion, while the second one is typical for the hopping conductance with a variable hopping length. It can be seen from the figure that, in the case of small oxygen deficiency and temperatures that are not too close to T_c, the dependence of $\rho_c(T)$ is better approximated by the first formula, while at the maximal oxygen deficiency, as well as near the transition to the superconducting state in the case of an intermediate oxygen content, the expression for hopping conductivity is better.

It can also be seen from the figure that the slope of the curves increases as the oxygen deficiency is increased, which in turn means that the activation energy also increases (see the Table). The slope of the curve with the minimal T_c changes with temperature, which in turn corresponds to a change of the activation energy from 38.45 to 14.5 and to 6.47 meV at 144 and 89 K, respectively, and reflects the presence of phase transitions observed earlier in work [1]. According to [1], phase transitions of this type affect kinetics of the charge transport. Thus, the analysis of the obtained experimental data allows us to assume that the decreas of the oxygen content leads to a localization of carriers in the direction of **c** axis and to a modification of the interlayer interaction.

In Fig. 2,*a*, the temperature dependences of the electroresistance in the *ab* plane $\rho_{ab}(T)$ measured after the sample annealing are shown for the same regimes and temperatures of the annealing as in the case of the previous sample. It is seen that in all cases the character of the conductivity at high temperatures remains quasimetallic. The absolute value of the

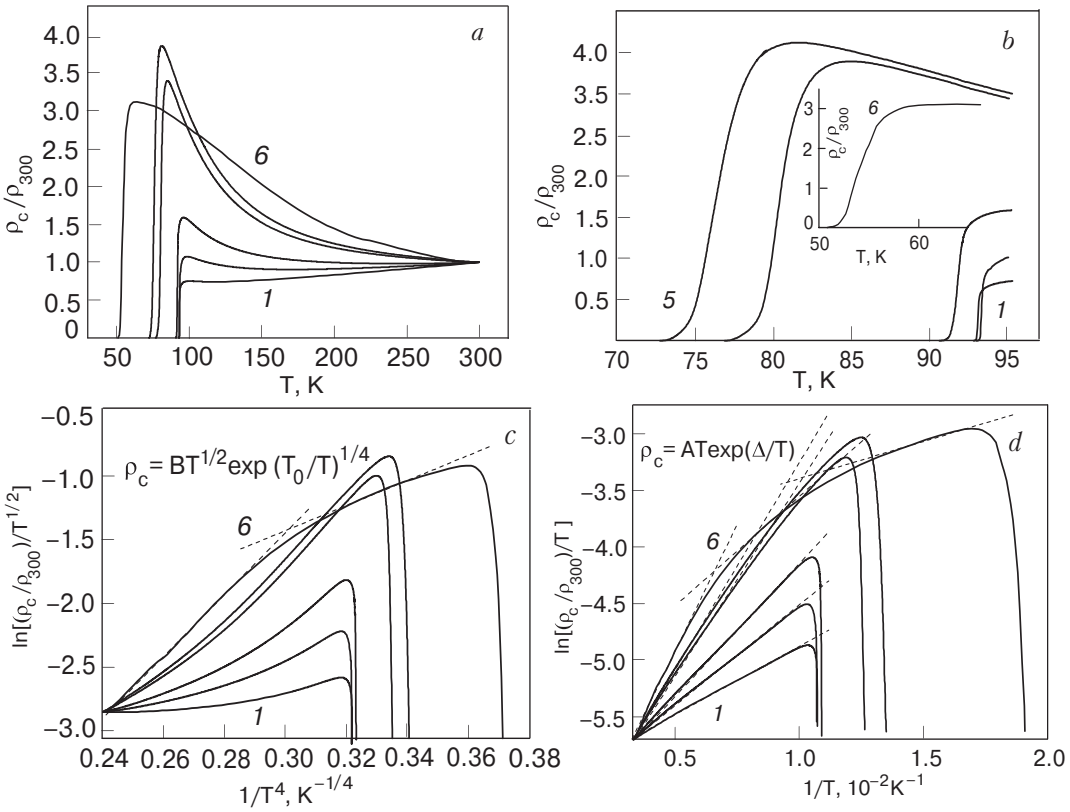

Fig. 1. The off-plane resistivity as a function of temperature in coordinates $\rho_c/\rho_{300}-T$ (*a*, *b*); $\ln[(\rho_c/\rho_{300})/T^{1/2}]-1/T^4$ (*c*) and $\ln[(\rho_c/\rho_{300})/T]-1/T$ (*d*) the superconducting transitions are shown. The curves *1–6* correspond to temperatures of annealing 670, 720, 760, 790, 810, and 890 K, respectively.

electroresistance increases, and the range, in which the dependence of $\rho_{ab}(T)$ is linear, becomes significantly narrowed.

It can be seen from the table and Fig. 2,*b* that, as the annealing temperature increases, the critical temperature decreases, the initial small width of the superconducting transition ($\Delta T_c \le 0.3$ K) significantly grows, and the transition acquires a step-like character. Also, it is worth noting that the height and the width of the bottom step increase with the annealing temperature, which is an obvious signature of the occurrence in the sample of two phases with different critical temperatures of the transition to the superconducting state. Because in the measurements of $\rho_c(T)$ the widest bottom step was not observed (see Fig. 1,*b*), it is logical to explain its existence in the $\rho_{ab}(T)$ curves by the suppression of superconductivity in twin boundaries. Indeed, the absence of a step in the dependences of $\rho_c(T)$ and its presence in the measurement of $\rho_{ab}(T)$ implies the presence of percolation routs for the transport current **I** in the high-temperature phase in the first case, when $\mathbf{I} \parallel \mathrm{TB} \parallel \mathbf{c}$, and their absence in the second case, when the angle between **I** and twin bondaries is 45°. At the same time, the increase of the step width with the increase of the annealing temperature means that the difference between the critical temperatures of the low- and high-temperature superconducting phases increases when the oxygen content decreases.

As follows from Fig. 2,*a*, at temperatures below some characteristic value T^* the dependences of $\rho_{ab}(T)$ «are rounded», which, apparently, may be due to the excess conductivity which temperature dependence can be derived directly from the equation:

$$\Delta\sigma = \sigma - \sigma_0, \qquad (2)$$

where $\sigma_0 = \rho^{-1} = (A + BT)^{-1}$ is the conductivity determined by the extrapolation of the linear part of the $\rho_{ab}(T)$ curves to zero temperature, and $\sigma_0 = \rho^{-1}$ is the experimentally measured value of the conductivity in the normal state. The temperature dependences of the excess conductivity are shown on Fig. 2,*c* and 2,*d* in coordinates $\Delta\sigma-T$ and $\ln\Delta\sigma-1/T$. It can be seen that, in a quite wide temperature interval, the dependences are well approximated by the expression

$$\Delta\sigma = \Delta\sigma_0 \exp(\Delta^*_{ab}/T), \qquad (3)$$

where $\Delta\sigma_0$ is an approximation constant, Δ^*_{ab} is a quantity determining some process of thermoactivation across an energy gap, also called «pseudogap».

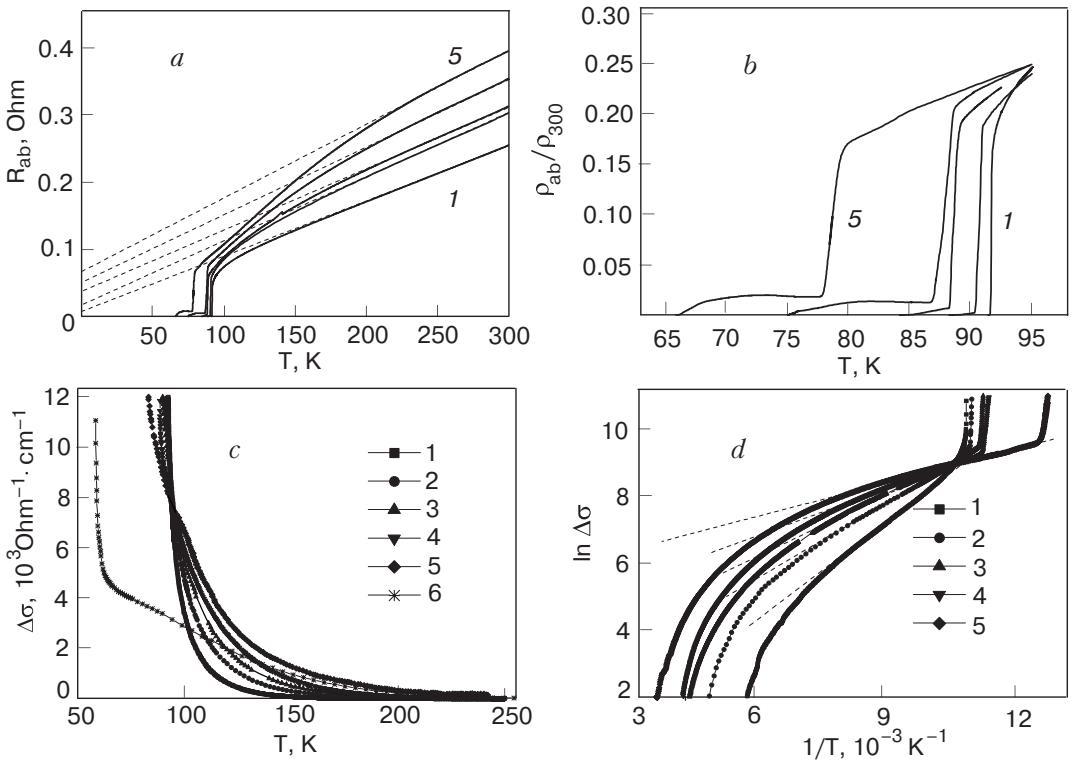

Fig. 2. The temperature dependences of conductivity in *ab* plane: resistivity as a function of T (*a*) and the superconducting transitions (*b*); dependences $\Delta\sigma$ vs T (*c*) and ln $\Delta\sigma$ vs $1/T$ (*d*). The numbering of curves corresponds to annealing temperatures given in Fig. 1.

The exponential dependence of $\Delta\sigma(T)$ has already been observed before for film [7], ceramic [8] and magnesium doped samples YBCO [9] with the comparable values of Δ^*. As it was shown in [7], the region of approximation of experimental data may be significantly expanded by adding factor $(1 - T/T^*)$. According to [7], the excess conductivity is proportional to the density of superconducting carriers n_s $(1 - T/T^*)$ and is inversely proportional to the number of pairs $\exp(-\Delta^*/kT)$ broken by the thermal motion. T^* is considered as the mean-field temperature of the superconducting transition, while the temperature interval $T_c < T < T^*$, in which the pseudogap state exists, is determined by the rigidity of the phase of the order parameter, which decreases as the oxygen deficiency increases.

In Fig. 3,*a*, the dependences of $\rho_{ab}(T)$ are shown for samples with the largest oxygen deficiency $\delta > 0.35$ and $T_c \approx 57$ and 45 K. In contrast to the cases with $\delta < 0.35$, a semiconductor-like part is clearly observed in the dependences at $T^* < 250$ K, while for the sample with the $T_c \approx 45$ K the linear part of the $\rho_{ab}(T)$ dependence has not been observed at all in the investigated temperature range. The temperature dependences of the excess conductivity of the sample with $T_c \approx 57$ K are shown in Fig. 3,*b* in coordinates $\Delta\sigma - T$ and $\ln\Delta\sigma - 1/T$. In comparison with Fig. 2,*c* and *d*, the linear part of the dependence $\ln\Delta\sigma(T)$ has increased almost twice, while the absolute value of the pseudogap has decreased by more than 30%. For the sample with $T_c \approx 45$ K, the the dependences of $\rho_{ab}(T)$ are well described by activation equations like $\rho_{ab} = \rho_0 \exp(\Delta/T)$ and $\rho_{ab} = \rho_0 T \exp(\Delta/T)$ (Fig. 3,*c*), as in the case of the experiment with $\mathbf{I} \| \mathbf{c}$. The value of Δ_{ab} obtained from the linear part of the dependence $\ln\Delta\sigma$ vs $1/T$ was about 6 meV, which is comparable to the minimal values obtained for Δ_c.

In Fig. 3,*d*, the concentration dependences of $\Delta^*_{ab}(\delta)$ and $\Delta_c(\delta)$ are shown. It can be seen that there is a clear correlation between the process of the energy gap evolution for the basic plane and for the direction of **c** axis upon the variation of the oxygen content. $\Delta^*_{ab}(\delta)$ and $\Delta_c(\delta)$ vary antisymmetrically. Δ^*_{ab} decreases while Δ_c increases, and vice versa. Thus, the analysis of the obtained experimental data allow us to draw a conclusion about suppression of the PG regime with a simultaneous amplification of the localization effects.

It can be seen from Figs. 2,*c* and 3,*b* that, when approaching T_c, there is a sharp increase of $\Delta\sigma$. It is known from the theory [10] that, in vicinity of T_c, the excess conductivity is caused by the processes of the fluctuating pairing of carriers (FC), whose contribu-

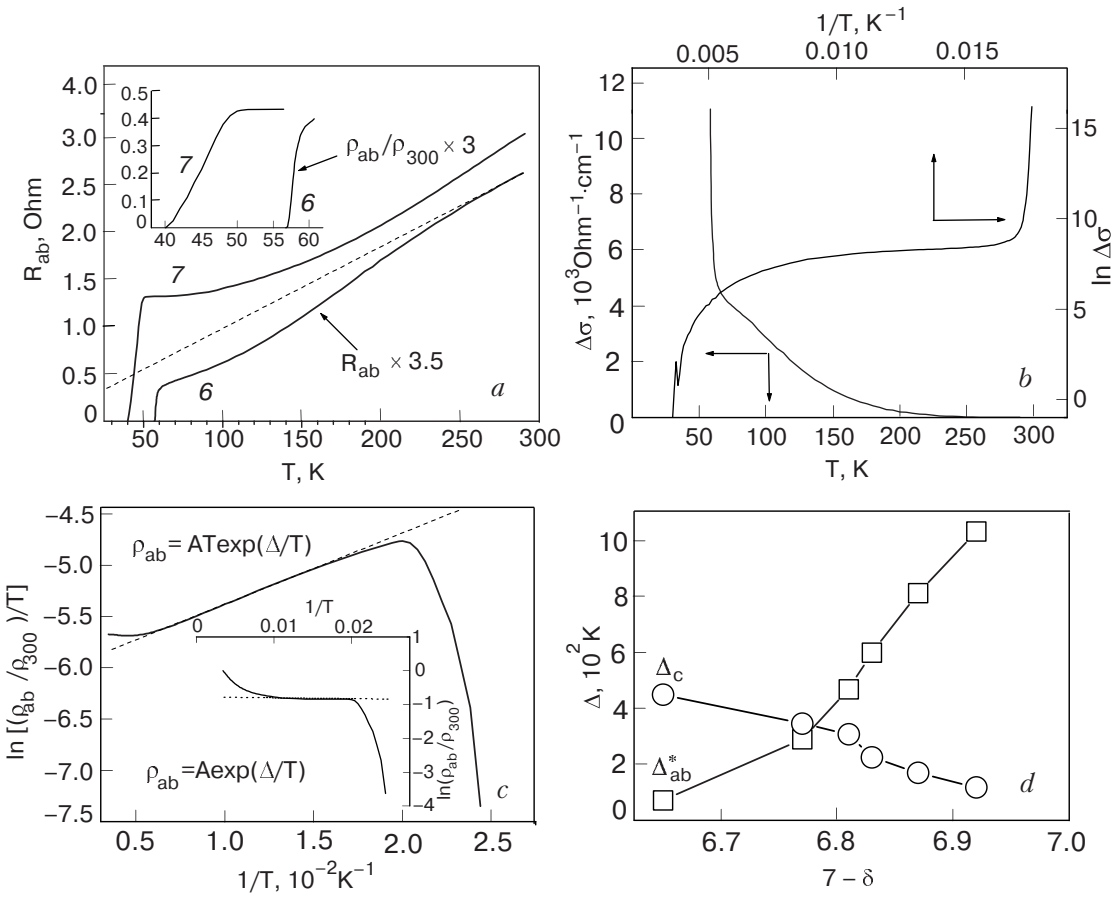

Fig. 3. a — In-plane resistivity as a function of T is shown for samples with the $T_c \approx 57$ and 45 K (curves *6* and *7*, respectively); inset: superconductivity transitions; *b* — temperature dependences of $\Delta\sigma$ vs T and $\ln \Delta\sigma$ vs $1/T$ for the sample with $T_c \approx 57$ K; *c* — temperature dependences of electroresistance for the sample with $T_c \approx 45$ K in coordinates $\ln [(\rho_{ab}/\rho_{300})/T] - 1/T$ and $\ln (\rho_{ab}/\rho_{300}) - 1/T$; *d* — dependences of the energy gap in the *ab* plane Δ^*_{ab} and along the **c** axis Δ_c as a function of δ.

tion to the conductivity at $T > T_c$ is determined by the power dependence [11]:

$$\Delta\sigma = \frac{e^2}{16\hbar d}\,\varepsilon^{-1}(1 + J\varepsilon^{-1})^{-1/2}, \qquad (4)$$

where $\varepsilon = (T - T_c)/T_c$ is the reduced temperature; T_c is the critical temperature; $J = (2\xi_c(0)/d)^2$ is the constant of interplane coupling; ξ_c is the coherence length along the **c** axis, and d is the thickness of the two-dimensional layer. In the two limiting cases (either close to T_c, where $\xi_c >> d$ and so the interaction between fluctuating Cooper pairs is realized in the entire volume of the superconductor — a 3D regime, or far from T_c, where $\xi_c << d$, and so the interaction is possible only in planes of the conducting layers — a 2D regime) expression (3) is reduced to known expressions for the three- and two-dimensional cases [10]:

$$\Delta\sigma_{2D} = \frac{e^2}{16\hbar d}\,\varepsilon^{-1}, \qquad (5)$$

$$\Delta\sigma_{3D} = \frac{e^2}{32\hbar\xi_c(0)}\,\varepsilon^{-1/2}. \qquad (6)$$

When fitting experimental data, the exact definition of T_c becomes particularly important. In our case, T_c was defined as the maxima of the high-temperature peak of the derivative $dR_{ab}(T)/dT$ in area of the superconductor transition [12].

A relationship between the $\Delta\sigma$ and the reduced temperature ε in coordinates $\ln\Delta\sigma - \ln\varepsilon$ are shown in Fig. 4. On these diagrams the 2D–3D crossover can be determined as transition from 3D regime ($\alpha_1 = d\ln\Delta\sigma/d\ln\varepsilon \approx -0.5$) to 2D regime ($\alpha_2 = d\ln\Delta\sigma/d\ln\varepsilon \approx -1.0$). As follows from (5) and (6), in the 2D–3D crossover point:

$$\varepsilon_0 = 4[\xi_c(0)/d]^2. \qquad (7)$$

In this case the value of the coherence length $\xi_c(0)$ can be calculated with equation (7) by inserting the values of crossover temperature ε_0 and d (as lattice constant $c = 11.7$ Å for samples with different oxygen contents [13]). However, it can be seen from the fig-

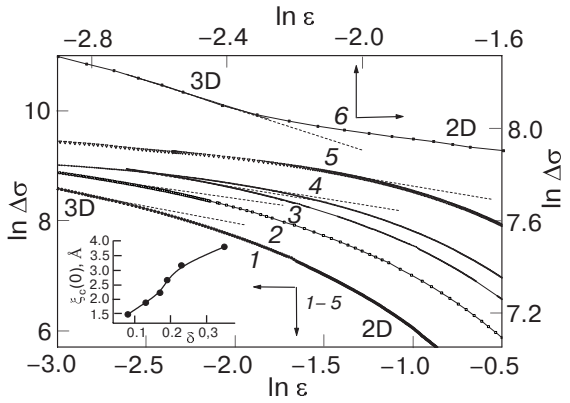

Fig. 4. The dependences $\Delta\sigma(T)$ in coordinates $\ln\Delta\sigma - \ln\varepsilon$. The numbering of the curves corresponds to that in Fig. 1. In the inset, the dependence of $\xi_c(0)$ versus the oxygen content δ is shown.

ure that for curve *6* ($\delta \approx 0.35$) there was no transition to 2D regime with expected slope $\alpha_2 \approx -1.0$. For this sample characteristic value of α_2 was about ≈ -0.25. According to [14], it may be an indication of the existence of the FC regime in the sample, which was proved for the first time in theoretical Maki–Thompson model [15] that assumes a domination of processes of scattering of fluctuating Cooper pairs by normal carriers. As was shown in [14], in the case of AL–MT crossover:

$$\xi_c(0)\varepsilon_0^{-1/2} \approx d \,. \qquad (8)$$

The dependence of $\xi_c(0)$ upon the oxygen content δ calculated by (7) and (8) is shown in the inset of Fig. 4. It can be seen that values of $\xi_c(0)$ increases from 1.48 to 3.8 Å as the oxygen deficiency is increased.

Having determined the temperature of transition to the FC regime T_f using the point of deviation of $\Delta\sigma$ upwards from the linear dependence (Fig. 2,*d*) at the temperature decrease, it is possible to estimate the relative extent of existence of the PG and FC regimes of the excess conductivity as $t^* = (T^* - T_f)/T_f$ and

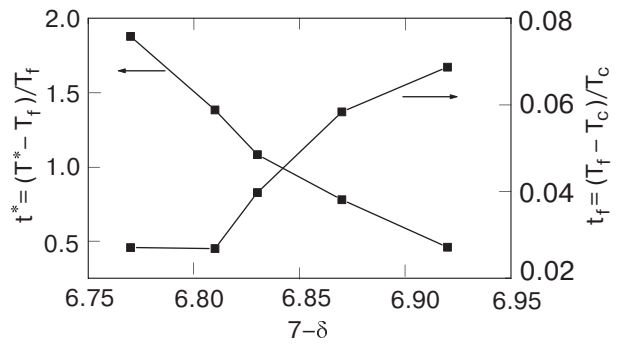

Fig 5. The dependences of the relative width of PG and FC regimes $t^* = (T^* - T_f)/T_f$ and $t_f = (T_f - T_c)/T_c$ as a function of δ.

$t_f = (T_f - T_c)/T_c$ [7], respectively. The results of calculation are shown in Fig. 5. It can be seen that, at a small oxygen deficiency $\delta < 0.35$, a general relative narrowing of the temperature intervals when FC is realized occurs whereas the temperature intervals when PG is realized expand.

In summary, the main results of the present work are: i) A decrease of the degree of the oxygen doping results in a transition from the metallic behavior of temperature dependences of conductivity along the **c** axis to the hopping conductivity with a variable length of hop; ii) In the case of the deficient oxygen content with $\delta > 0.35$, phase transitions at 144 and 89 K change the activation energy of the charge transfer along **c** axis; iii) In the *ab* plane, the decrease of oxygen content results in a significant narrowing of the interval of the linear $\rho_{ab}(T)$ dependence and in an expansion of the interval in which the pseudogap regime is realized; at the same time, the excess conductivity is described by exponential temperature dependence in a wide temperature range; iv) When the oxygen content is varied, the absolute values of the in-plane and off-plane energy gaps change with different signs of their derivatives. When the value of Δ_c increases, the value of the pseudogap Δ^*_{ab} decreases; v) The expansion of the interval of realization of the pseudogap regime results in a relative narrowing of the temperature interval, in which regime of the fluctuation conductivity is realized.

1. M.A. Obolenskii, A.V. Bondarenko, V.I. Beletskii, V.N. Morgun, V.P. Popov, N.N. Chebotaev, A.S. Panfilov, A.I. Smirnov, O.A. Mironov, S.V. Chistyakov, and I.Yu. Skrylev, *Fiz. Nizk. Temp.* **16**, 1103 (1990) [*Low Temp. Phys.* **16**, 639 (1990)].
2. M.A. Obolenskii, A.V. Bondarenko, R.V. Vovk, and A.A. Prodan, *Fiz. Nizk. Temp.* **23**, 1178 (1997) [*Low Temp. Phys.* **23**, 882 (1997)].
3. B.P. Stojkovic and D. Pines, *Phys. Rev.* **B55**, 8567 (1997).
4. T. Ito, K. Takenaka, and S. Uchida, *Phys. Rev. Lett.* **70**, 3995 (1993).
5. M.V. Sadovskii, *Phys.-Usp.* **44**, 515 (2001).
6. P. Pieri, G.C. Strinati, and D. Moroni, *Phys. Rev. Lett.* **89**, 127003 (2002).
7. D.D. Prokof`ev, M.P. Volkov, and Yu.A. Boyko, *Fiz. Tverd. Tela* **45**, 1168 (2003).
8. A.F. Prekul, V.A. Rossohin, A.B. Rol'schikov, N.I. Schegolihina, and S.V. Yartseva, Sverhprovodimost': *Fizika, Khimiya, Tekhnika* **3**, 381 (1990).
9. Anand Vyas, C.C. Lam, and L.J. Shen, *Physica* **C341–348**, 935 (2000).
10. L.G. Aslamasov and A.I. Larkin, *Fiz. Tverd. Tela (Leningrad)* **10**, 1104 (1968) [*Sov. Phys. Solid State* **10**, 875 (1968)].

11. W.E. Lawrence and S. Doniach, *Proceedings of the 12th International Conference on Low Temperature Physics, Kyoto, Japan, 1970*, Keigaku, Tokyo (1970), p. 361.
12. L. Mendonca Ferreira et al., *Phys. Rev.* **B69**, 212505 (2004).
13. I.V. Aleksandrov, A.F. Goncharov, and S.M. Stishov, *Pis`ma Zh. Eksp. Teor. Fiz.* **47**, 357 (1988).
14. A.L. Solovyov, H.-U. Habermeier, and T. Haage, *Fiz. Nizk. Temp.* **28**, 24 (2002) [*Low Temp. Phys.* **28**, 20 (2002)].
15. J.B. Bieri, K. Maki, and R.S. Thompson, *Phys. Rev.* **B44**, 4709 (1991).